FORMULATION AND VALIDATION OF A POPULATION BALANCE MODEL FOR POWDER MIXING PROCESS

By

JOYCE JOHN

A thesis submitted to the

Graduate School – New Brunswick

Rutgers, The State University of New Jersey

in partial fulfillment of the requirements

for the degree of

Master of Science

Graduate Program in Chemical and Biochemical Engineering

Written under the direction of

Dr. Rohit Ramachandran

and approved by

_____

_____

_____

_____

New Brunswick, New Jersey

May, 2013

ABSTRACT OF THE THESIS

Formulation and validation of a population balance model for powder mixing process

by Joyce John

Thesis Director: Dr. Rohit Ramachandran

Pharmaceutical processing is much more stringent with regulatory requirements for the processing and handling stages and the product quality specifications must be met at every step during the manufacturing operation. In the pharmaceutical manufacturing, the unit operation that is one among the most widely used, is the powder blending operation. The scope of this work is to characterize and document the complex powder blending process by means of a robust predictive model and use it to enhance operational efficiency and improve on the established monitoring and control strategies.

The implementation of QbD (Quality by Design) strategies [1] to continuous processing stages allows for improved process control, higher cost-efficiency without compromising on the quality or efficacy of the final product. It also would alleviate the need for further scale up studies. In this work, a population balance model (PBM) has been formulated and validated to model the complex dynamics within a continuous powder mixing process, with the focus on the blending operation taking place within pharmaceutical tablet manufacturing. PBM modeling was selected to model the blending unit operation as it not only serves as a dynamic and highly effective tool, but also due to its relative computational simplicity.

The model was designed to determine the critical quality attributes (such as RTD (residence time distribution), API composition and RSD (relative standard deviation) of the product by incorporating the key process parameters such as the impeller RPM, dimensions of the blender and design parameters such as the number of compartments (both axial and radial), etc. The model obtained has been subsequently validated to check the fit between the predicted values of these CQAs (Critical Quality Attributes) against experimentally obtained data during the same time intervals. The model has the potential use for process improvement by implementation in a PAT (Process Analytical Technique) system for designing improved monitoring, control and optimization techniques. [2]

Acknowledgements

This is a feeble attempt to thank everyone who has made my life and work at Rutgers an unforgettable experience.

First and foremost, I would like to thank my thesis advisor, Dr. Rohit Ramachandran for showing immense support and guidance throughout the course of my research work at Rutgers. I would particularly like to thank the other members of my thesis committee: Dr. Meenakshi Dutt, Dr. Aditya Vanarase, and Dr. Xue Liu for their time, interest and valuable suggestions. I would also like to express my sincere appreciation to all the faculty and staff at Rutgers University that I have had the pleasure to interact with.

My heartfelt gratitude to my colleagues Maitraye Sen, Anwesha Chaudhury, Anuj Varghese and Dana Barrasso and many others for your invaluable help and insight that was instrumental in the completion of my research work.

I am greatly indebted to the people who made my stay at Rutgers a wonderful and cherishable one - my fellow group members, roommates and friends in and out of the CBE family.

Lastly, but most importantly, my family for instilling a deep sense of faith in me and for believing in me at all times. Thank you all for the giving me so many memories, I shall be ever grateful.

Dedication

"He that dwelleth in the secret place of the most High shall abide under the shadow of the Almighty. I will say to the Lord, He is my refuge and my fortress: my God: in Him will I trust."

- Psalms 91: 1, 2

This work is dedicated to my Lord and Savior, Jesus Christ for giving a purpose and meaning to my life, and, to my wonderful, one- of- a kind family.

Table of Contents

List of Figures

List of Tables

Chapter1

Introduction

In the pharmaceutical industry, the regulatory environment nature is much more stringent than in any other process industry, in terms of process operation, handling and final product requirements in terms of purity, efficacy and quality. [3] Powder feeding, blending, milling, granulation, tableting and coating are the typical continuous processing stages used for the production a pharmaceutical oral solid dosage form. It is important to have a sound understanding of each and every one of these unit operations in order to achieve the desired operation level. Among these processes, powder blending operation, is probably the most basic and extensively used unit operation. The unpredictability of this process is primarily due to the lack of understanding between the material properties and it's relation to process performance, due to which each drug formulation is considered unique from the rest. To overcome this challenge, a quantitative method was preferred over an empirical methodology to get a more accurate prediction. In addition, non-predictive effects of process models or inefficient control strategies could result in high degree of variability within the process and the product may fail to meet the required specifications. [4, 5] The characterization by means of a robust predictive model to explain the complex dynamic behavior occurring within the mixer is essential for improving the design, monitoring, analysis and control of the process.

Powder mixing is the act of bringing bulk material within intimate contact with one another so as to obtain a uniform blend consistency. [6] The blending primarily occurs as a combined result of convective and diffusive velocity gradients produced within the mixer. It is regarded as one of the most important unit operations since it decides the final product composition, uniformity and consistency.

The predictability of the behavior within of powder processing units, especially in granular flow is still rudimentary and this attributed to the lack of governing equations under specified conditions. In this operation, the bulk nature is decided by the highly chaotic micro-scale particle interaction but due to the lack of specific equations, the particle- particle and particle –blender wall interaction is a bit more tedious to analyze and results in complexity of the model. As a result, most pharmaceutical process developers resort to a uni-variate trial and error methodology which is both expensive and time consuming since it is a multi- variable complex process. [2]

The FDA (Food And Drug Administration) highly recommends the implementation of QbD (Quality by Design) principles alongside PAT (Process Analytical Technology) tools [7, 8, 9, 10, 11, 12, 13] for process monitoring by either in-line, at-line or off-line sensing. It serves to improve not only the process, but also its monitoring and control by performing a holistic risk based assessment of both the product and the process. Quality by design principle employs the design space concept in which predictive modeling is carried out in which the inputs such as equipment variations and other manufacturing inputs are kept within an acceptable range so that the product obtained is well within the

required specifications. [3, 14] PAT tools ensures timely monitoring and analysis of the system by monitoring the CPPs (Critical Process Parameters) affecting the Critical Quality attributes (CQA) of the product. This in-line/off line sensing allows for a timely intervention by process alteration or control to be carried out in case of inconsistency during product formation, reduces losses due to production of rejects/ineffective. This is crucial in operation of large plants as a well-timed sensing and intervention eliminates the need to carry out further corrective processing stages and subsequent loss of time, cost and labor. It also ensures higher test efficiency and consistency in product formation. [11, 15]

Regulatory authorities and pharmaceutical manufacturers are lately noting a shift in trend from frozen batch processes towards developing equation based continuous processing techniques for drug design and development. Most of the established processes in the industry are batch processes, and any transition would require process remodeling, revalidation and regulatory approval, all of which require time and money. In addition, there is also an age-old and popular mindset that only batch processes deliver products meeting product specifications. This notion is slowly changing. The use of continuous mode of operations makes further scale up easier as the same equipment can be used for large and small scale operations [5], additionally the lesser plant area requirement allows a reduced plant footprint and is much more environment- friendly. [16, 17, 18, 19] It also enables us to get higher yields in theory and is considered to be less labor intensive and much more energy efficient. [14, 19, 20, 21, 22, 23, 24] It is noted that among the batch

processes, those that have multi-purpose equipment incorporated operate more efficiently in comparison with single-purpose equipment [25, 26, 27].

Though there are several noted advantages to shifting to continuous mode, the relative complexity of the process for processes involving several variables poses a major drawback to process understanding and control. If the parameter estimation or process prediction fails or ineffective control mechanisms [4, 5] are employed, the losses incurred from a continuous mode may be far more than a batch mode of operation. [2, 28] In addition continuous mode of operation means the equipment maintenance and cleaning will be more expensive as the setup must be dismantled, cleaned and reassembled [14], which requires skilled manpower and poses time constraints. Flow sheet modeling of continuous processes can be performed which enables it to be accurately designed, optimized and can be used for simulating the functioning of a real plant [12].

In pharmaceutical blending process that deals with fine cohesive powders, the prime reason for blend inconsistency is largely attributed to aggregation and segregation, which can occur within the mixer. These phenomena cause smaller particles to form agglomerates under the presence of cohesive forces. It prompts particle segregation due to differences in the mobility of the agglomerates, thereby affecting the homogeneity [6]. Segregation causes the separation of distinct particles within the blender resulting in blend inconsistency and quality issues. A design space concept can provide an efficient framework for modeling the complete dynamics within the blender. In this technique, all the parameters considered should lie within a well-defined design space. This technique

can improve cost, time and labor efficiency of process and product development. [7, 29, 30, 31]. Software programs such as gPROMS^{TM} (Process systems enterprise), GAMS (GAMS Development Corporation), DEM (Discrete Element Modeling), etc. are used for this purpose. [2]

The continuum and constitutive models [25], statistical models [32, 33, 34], the Monte-Carlo methods [35], compartment models [36, 37], RTD models [38, 39, 40, 41], DEM [41], hybrid models [43, 44] are some of the modeling techniques in use today. Among these DEM (Discrete Element Modeling) technique is the most fundamental modeling approach that describes particle level physic, by considering each particle as a discrete entity. It allows us to track the individual particle trajectories and particle collisions can be modeled. Each particle's motion (translational or rotational) is based on Newton's Laws of Motion. In DEM, a finite number of particles are considered to interact via several contact and non- contact forces. [2, 45]

From literature we can see documented work done on the dynamics of mixing [2, 46, 47, 48, 49, 50, 51, 52, 53, 54] towards understanding the bulk flow and particle behavior occurring within the blender. In order to study the fluid-particle interactions, DEM was coupled with computational fluid dynamics [2, 55, 56, 57]. DEM method was also used to study the blending dynamics of different blender types such as rotational mixers [58, 59, 60, 61, 62], helical mixers [63, 64, 65, 66] and rotor type mixers [67, 68, 69, 70], etc.

Though DEM has been extensively used to study and model blending behavior, there is still potential for work to be done in characterizing the dynamic behavior of granular materials and the nature of particle-particle or particle-fluid interactions, especially for blenders handling cohesive powders. It can be noted that PBM has been employed to study the flow properties of processes such as crystallization [71, 72, 73, 74] and granulation [75, 76, 77, 78, 79, 80, 81, 82, 83]. There is scope for work to be done towards introducing PBM modeling for blending. The framework has been validated using experimental data and subsequent statistical analysis of the results was conducted. The population balance framework has several advantages such as it is computationally less time consuming than DEM modeling alone. [2, 84, 85]

1.1. Objective

The reported work has been aimed at developing a novel and dynamic multi-dimensional PBM framework for blending process. The model has been validated against experimental data. Since the model involved several parameters, detailed optimization based parameter estimation has been carried out to obtain their optimum values. The optimization framework has been formulated on GAMS (General Algebraic Modeling System) which is a robust modeling optimization tool. The flux ratios between any two compartments have been estimated after optimizing the critical quality attributes (RSD, RTD and API composition).

Chapter 2

Systematic Framework

It is very important to identify which critical process variables are to be optimized in order to validate the model. There were several stages which are used to develop this model- optimization framework and the first stage involves structuring the problem definition in terms of the process specifications. The purpose of such a detailed framework is to develop a mathematical model representing a continuous blending operation. In order to do so the blender has been divided into several compartments or bins. Mass balance equations are used to express the powder flow among these compartments. The parameters that need to be estimated should then be identified and for our model, we have considered the flux ratios as the key parameters to be estimated. Owing to the dynamic nature of the model, the parameters need to be estimated for each point of time.

The CQA (Critical Quality Attributes) of the blend such as the RTD (Residence Time Distribution), the API composition and the RSD (Relative Standard Deviation) are the variables used to evaluate the blending performance. A series of experiments were carried out in order to obtain data sets of these variables as a function of time. The next stage involves the selection of the proper optimization tool. The time required to run the optimization program is the most important consideration due to the multi-dimensional and dynamic nature of the problem. Hence the optimization framework has been solved using a built-in solver within the software called GAMS (General Algebraic Modeling

System). The designed model has been validated against experimental data sets. The model shows considerable accuracy in tracking these data. Figure 1 is the schematic representation of the steps which were followed. [2]

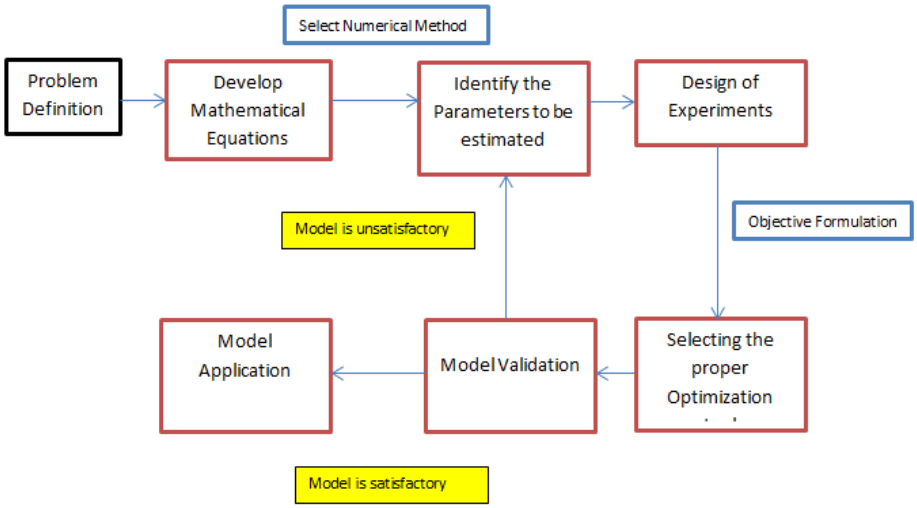

Figure 1: Schematic of optimization framework

Chapter 3

Model Description

This section provides a brief description of how the model has been formulated mathematically.

3.1. Population Balance Model (PBM)

The Population Balance Equation which was used was adapted from [86]:

$$\frac{\partial}{\partial \mathrm{t}}\mathrm{F}(\mathrm{x},\mathrm{z},\mathrm{t}) + \frac{\partial}{\partial \mathrm{x}}\left[\mathrm{F}(\mathrm{x},\mathrm{z},\mathrm{t})\frac{\mathrm{dx}}{\mathrm{dt}}\right] + \frac{\partial}{\partial \mathrm{z}}\left[\mathrm{F}(\mathrm{x},\mathrm{z},\mathrm{t})\frac{\mathrm{dz}}{\mathrm{dt}}\right] = \mathrm{R}_{\mathrm{Formation}} - \mathrm{R}_{\mathrm{Depletion}} \quad (1)$$

F(**x**, **z**, t) is the population distribution function, **x** is the vector of internal coordinates used to express the particle size and **z** is the vector of external co-ordinates used to represent spatial position of the particles and t is the time. The term $\frac{\partial}{\partial x}\left[F(\boldsymbol{x},\boldsymbol{z},t)\frac{dx}{dt}\right]$ accounts for the rate of change of particle distribution due to change in particle size. The term $\frac{\partial}{\partial z}\left[F(\boldsymbol{x},\boldsymbol{z},t)\frac{dz}{dt}\right]$ accounts for the rate of change of particle size distribution with respect to spatial co-ordinates. Particles are formed due to nucleation, aggregation and breakage phenomena. $R_{Formation}$ and $R_{Depletion}$ stand for particles being formed and depleted respectively due to the above mentioned phenomena. In this case, we have assumed no size change occurring (either by breakage or formation) since we are considering mixing of non-cohesive particles. [2, 14] The PBM after modification is given as:

$$\frac{\partial}{\partial t}[F(\boldsymbol{z},t)] + \frac{\partial}{\partial z}\left[F(\boldsymbol{z},t)\frac{dz}{dt}\right] = 0 \quad (2)$$

3.2. Mixing Model Formulation

The equation for blending can be written as:

$$\frac{\partial F(n,x,y,t)}{\partial t} + \frac{\partial}{\partial x}[F(n,x,y,t)\ dx/dt] + \frac{\partial}{\partial y}[F(n,x,y,t)\ dy/dt] = Inflow - Outflow \quad (3)$$

Here x is the spatial co-ordinate in the axial direction, y is the spatial co-ordinate in radial direction, n is the counter representing number of components and t is the time. In this model two components namely a single API and excipient are used, hence n=1 represents the API and n=2 represents the excipient.

Cartesian coordinates were used instead of polar coordinates since we are neglecting the curvature term from our model. The terms dx/dt and dy/dt represent the axial and radial fluxes respectively. The axial flux can be categorized as forward or backward flux. Forward axial flux will move the particles to the next compartment whereas the backward flux will move the particles to the previous compartment. Inflow is the feed rate of components into the mixer. If we are considering m x m compartments within the blender, then the outflow term will be $\sum_{n=1}^{2}\sum_{y=1}^{m} F(n,m,x_{max},y,t)V_f$. It is the particle number flux and has units of no. of particles/m^2s. Here V_f represents the forward flux term (m/s) and F is particle density (no. of particles/m^3). The value of n in the mixing

model can be changed in order to represent the mixing of more than 2 components within the blender. [2]

3.3. Modeling Methodology of the Blender

The blender has been divided into several compartments or bins. Mixing occurs as a result of convective and dispersive forces, but in this case the mixing taking place as a result of dispersion has been ignored. Mixing due to dispersion is due to spatial concentration gradient within the blender and convective mixing is due to the mechanical movement of the blades or any other movable parts of the blender. A literature review has been conducted prior to this work and it has been seen that dispersive term is very less than the convective term based on the work reported by Portillo et al. 2008. Hence in this model a similar assumption has been adopted and the mixing occurring as a result of dispersion is neglected. The blender considered here is cylindrical with rotating blades. As the motion of the blades is mainly responsible for moving the powder in the system hence the assumption is justified.

The particles are considered as discrete entities moving from one compartment to another resulting in an exchange of mass between the compartments. This has been represented as the particle number. Particles can either move forward to the compartment lying ahead of it or backward to the one behind it. In comparison, at fixed axial location, radial mixing conserves the total number of particles. This model inputs are only the flux values, which are a function of particle diameter, density and geometry, hence these information do not need to be supplied to the model. The values of the flux terms are determined

experimentally. Since these values vary with spatial position and particle type, for the optimization framework, they have been replaced by flux ratios. Flux ratio is defined as the ratio of the fluxes of any two compartments between which particle transfer occurs and it is used to denote the relative number of particles interchanged between any two compartments. For axial flux ratios, it assumes values of -1 (backward flux) and 1 (forward flux). Here we have used an assumption that 50% of the mass flux from any radial compartment moves to the compartment above it and 50% move to the compartment below it. In this model we have considered the average radial flux; hence it takes a value between 0 and 1. [2]

For a single component, the mass balance can be simplified according to the equation given below:

$$\frac{\partial F(x,y,t)}{\partial t} = \frac{V_f[F_{x-1,y,t} - F_{x,y,t}]}{\Delta x}\Delta t + \frac{V_b[F_{x+1,y,t} - F_{x,y,t}]}{\Delta x}\Delta t + V_r\frac{[F_{x,y+1,t} + F_{x,y-1,t} - 2F_{x,y,t}]}{\Delta y}\Delta t \qquad (4)$$

Here V_f , V_b , V_r denotes the forward, backward and radial flux terms respectively.

The critical quality attributes (CQA) namely the API composition, residence time distribution (RTD) and relative standard deviation (RSD) can be defined as given below.

The composition of the final mixture in terms of mean API composition y_{API} is given as:

$$y_{API} = \frac{\sum_{y=1}^{y_{max}} F(API, x_{max}, y, t)}{\sum_{n=1}^{n_{max}} \sum_{y=1}^{y_{max}} F(n, x_{max}, y, t)} \qquad (5)$$

In the above equation, the numerator and denominator represents the total number of API particles and the total number of both API and excipient particles coming out of the last compartments, respectively, at any point of time. x_{max} and y_{max} represents the maximum number of grids in the axial and radial directions respectively. Since we have considered only 2 components the value of n_{max} is 2.

The RSD is used as a measure of the degree of blend homogeneity and it is calculated by use of a tracer. The homogeneity of samples retrieved from the outflow is measured by calculating the variability in the tracer concentration. The Relative Standard Deviation (RSD) of the tracer concentration is given as:

$$RSD = \frac{\sqrt{\sum \frac{(y_i - y_{avg})^2}{(n-1)}}}{y_{avg}} \tag{6}$$

Residence time distribution (RTD) is a measure of the time spent by the fluid elements within the blender. It is denoted as E(t). In other words it captures the non-ideality associated with the flow. RTD can be found as:

$$E(t) = \frac{yAPI(t)}{\int_0^\infty yAPI(t)dt} \tag{7}$$

3.4. Numerical Technique

The entire system is discretized into several sub-groups or sub-populations and the population distribution function is formulated for each of these semi-lumped sub-groups. A finite volume technique is used for the discretization.

The population balance equation has been integrated over the domain of the sub-groups and then re-cast into finite volumes. The integro partial-differential equation is then reduced to a set of ODEs (ordinary differential equations) which can then be integrated using first order Euler method. [2, 80]

Chapter 4

Experimental Set-up

This section provides a brief discussion on the methodology adapted to obtain experimental data for model validation studies. The experimental set-up has been adopted from the work of Vanarase et al. [85]

4.1. Process and Equipment Description

The continuous mixer used for the study has been manufactured by Gericke (Model GCM 250) having a length and diameter of 300 mm and 100 mm respectively with alternately arranged blade set. Twelve triangular shaped blades are mounted on the impeller with equal spacing in between and an angle of 20 degrees. Few blades are forward facing which would move the powder forward while the rest are backward facing which would move the powder in reverse direction. A semicircular disc or weir is placed at the exit in order to control the fill level of the powder or the powder hold-up in the mixer. The weir angle is maintained at 20 degrees. The feeders used are Loss-In-Weight (LIW) type, manufactured by Schenck AccuRate. The two components namely the API and excipient particles are being continuously fed as two inlet streams. The blended product is being continuously withdrawn at the outlet. [2, 85]

4.2. Materials and Methods

Materials used for the experiment are Avicel PH-200 (FMC biopolymer) and Acetaminophen (Mallinckrodt). Here Avicel PH-200 and Acetaminophen are the

excipient and API respectively. Pure Acetaminophen is highly cohesive in nature, therefore it has been pre-blended with 0.25% of silicon dioxide to reduce its stickiness and improving flowability. A Nicolet Antaris NIR spectrometer (Thermo Fisher) has been used for sampling. ‘TQ Analyst’ has been used for calibration model development. Spectral data is thus obtained using the software ’Omnic’. Spectral data has been filtered using a Norris derivative filter. The value of coefficient of correlation (R^2) and root mean squared error of prediction (RMSEP) was 0.9831 and 0.239 respectively. These values indicate a good fit of the spectral data. [2, 85]

4.3. RTD Measurement

Avicel has been fed into the system until steady state has been achieved, following which, Acetaminophen is introduced into the inlet stream in the form of an instantaneous pulse. The tracer concentration at the outlet is maintained well above the detection limits of the NIR method. Samples are collected and analyzed by NIR spectroscopy at different time points and this experimental data collected was used for model validation studies. [2, 85].

Chapter 5

Parameter Estimation and Optimization

The optimization framework has been solved using GAMS. Since RTD is a different set of experiment, hence the RTD data has been fitted separately. The blender optimization model is non-linear with 10101 number of constraints and 22561 number of variables. The Hessian of the Lagrangian has 5800 elements on the diagonal, 37256 elements below the diagonal and 19660 nonlinear variables. [2]

The solver chosen is CONOPT, which is a non-linear programming algorithm software available on GAMS and it is effective for handling large and sparse model. CONOPT follows a non-linear programming algorithm based on a generic GRG (Generalized reduced gradient) algorithm. The details of this algorithm have been explained by A. Drud [86, 87]. Since the model is likely to have multiple solutions, hence initial guesses have been provided so that the solution can be obtained in an appropriate region. This also reduces the time involved in finding the feasible solution. The objective function has been scaled in order to fix good search directions.

The run time for the simulation is set at 100seconds. The blender has been divided into a 5 x 5 compartment system with a total of 25 compartments. The flux ratios are classified into three namely forward, backward and radial fluxes. Therefore there are a total of 15000 flux ratios to be estimated. [2]

5.1. Parameter Estimation

The dynamic population balance model after discretization can be represented as [80]:

$$\mathbf{y}(t,\mathbf{p}) = f(\mathbf{y}(t,\mathbf{p}),\mathbf{p}), \forall\, t\ \varepsilon\ (0, tf) \quad (8)$$

$$\mathbf{y}(0,\mathbf{p}) = y_o \quad (9)$$

Where y is the population distribution function and p are the model parameters. The model parameters in this case are the forward, backward and radial flux ratios between any two compartments.

Least square fitting has been used for parameter estimation. The objective is to decrease the squared error between the models predicted $x_{predicted}$ and the experimental data x_{expt}. The data are usually the RSD and API composition measured at different time points and they can be obtained by the algebraic manipulation of the states such that x(t, p)=g (y(t,p)).

The objective function can be formulated as shown below:

$$\Omega(p) = \sum_{i=1}^{n} \left\| x_{predicted}\ (t_i, p) - x_{expt}\ (t_i, p) \right\|^2 \quad (10)$$

Where n is the total number of points.

Gradient based optimization techniques are used to minimize Ω. The model sensitivities $\frac{\partial y_j}{\partial p_k}$ are integrated along with the model states **y** over the time domain, which are given as shown below:

$$\frac{\partial y}{\partial p}(t,p) = \frac{\partial f}{\partial y}(t,p)\frac{\partial y}{\partial p}(t,p) + \frac{\partial f}{\partial y}(t,p),\ \forall t\ \varepsilon\ (0,t_f) \quad (11)$$

$$\frac{\partial y}{\partial p}(0,p) = 0 \quad (12)$$

5.2. Objective Function Formulation

The RSD and API composition data were obtained from the experiments. The RSD and API composition have values of different orders. Therefore the objective function for RSD is multiplied by a constant k to facilitate convergence. Individual objective functions can be formulated for each of the critical quality attributes as shown below:

$$\Omega_{API\ composition}(p) = \sum_{i=1}^{n} \left\| y_{API\ predicted}(t_i,p) - y_{APIexpt}\ (t_i) \right\|^2 \quad (13)$$

$$\Omega_{RSD}(p) = \sum_{i=1}^{n} \left\| RSD_{\ predicted}(t_i,p) - RSD_{\ expt}\ (t_i) \right\|^2 \quad (14)$$

The overall objective function can then be formulated as:

$$\Omega^{Total}(p) = \Omega^{RSD}(p) + \Omega^{APIcomposition}(p) \quad (15)$$

Since RTD measurement is a completely different set of experiment, hence the objective function has been formulated and optimized separately as shown in:

$$\Omega^{RTD}(p) = \sum_{i=1}^{n} \left\| E_{predicted}\ (t_i,p) - E_{experimental}(t_i) \right\|^2 \quad (16)$$

$$\sigma(t) = \frac{y_{API}(t)}{\int_0^\infty y_{API}(t)dt} \quad (17)$$

5.3. Statistical Analysis

In order to test the robustness of the model, statistical tests have been conducted. A brief discussion on the various statistics which we considered in order to understand how effectively the model can fit the experimental data have been provided below.

The Pearson correlation coefficient (R): The correlation coefficient measures the strength of a linear relationship or the degree of association between the model predicted and experimental data. It can take any value between -1 and +1. A value of +1 will indicate a straight line between the experimental and predicted data.

$$R = \frac{\sum_{i=1}^{n}(xi-x)(yi-y)}{\sum_{i=1}^{n}(xi-x)^2 \sum_{i=1}^{n}(yi-y)^2} \quad (18)$$

Error sum of squares (SSE): It is a measure of the accuracy of predictions from model. Lower the value, better the model.

$$SSE = \sum(y_i - x_i)^2 \quad (19)$$

Regression sum of squares (SSR): It is another measure for predicting the accuracy of the model.

$$SSR = \sum(xi - y)^2 \quad (20)$$

Coefficient of correlation (R^2) and adjusted R^2: It gives the extent of variance or fluctuation of the predictable variable. It is a measure of the certainty with which predictions can be made from the model. It can take any value between 0 and 1. If R^2 is equal to 1, it will indicate that regression line perfectly fits the data. However a large value of R^2 does not always imply that the model is a good one. For example, adding a variable to the model will always increase the value of R^2 regardless of whether the additional variable is statistically significant or not. To overcome this drawback, adjusted R^2 is often used. Its value is not affected by addition of any new variable to the model. Adjusted R^2 has the same significance as the R^2.

$$R^2 = 1 - \frac{SSE}{SST} \quad (21)$$

Where $SST = \sum(y_i -)^2$

Chapter 6

Results and Discussion

Data have been collected by varying the blender speed. Mixer RPM is one of the important processing parameters as far as the blend quality is concerned. Mixer RPM affects the degree of axial and radial mixing. Residence time distribution model has been formulated and validated separately. RTD (Residence Time Distribution) decreases with increase in mixer RPM. Whenever a process is started, the system stays in unsteady state initially and then reaches steady state gradually. Usually the product obtained during unsteady state is discarded. But in this work the entire dynamics of the system has been considered starting from time t=0 to final end time point. Therefore none of the experimental data points have been neglected.

It can be seen that the experimental data sets are chaotic. This may be due to the presence of certain non-idealities in the system (i.e. clogging of particles due to poor equipment geometry, wear and tear etc.) or measurement errors.

This model has been developed for a generalized mixing operation for free flowing powders (no aggregation or coagulation are present) and hence no non-ideality has been introduced in the model. Therefore a polynomial trend line has been fitted to the experimental data sets to obtain a smooth response. The averaging function for the trend line is an nth degree polynomial where n=2 or 3. The model is validated for the fitted trend line. The model simulations were performed on an 8GB RAM, 2.94 GHz desktop.

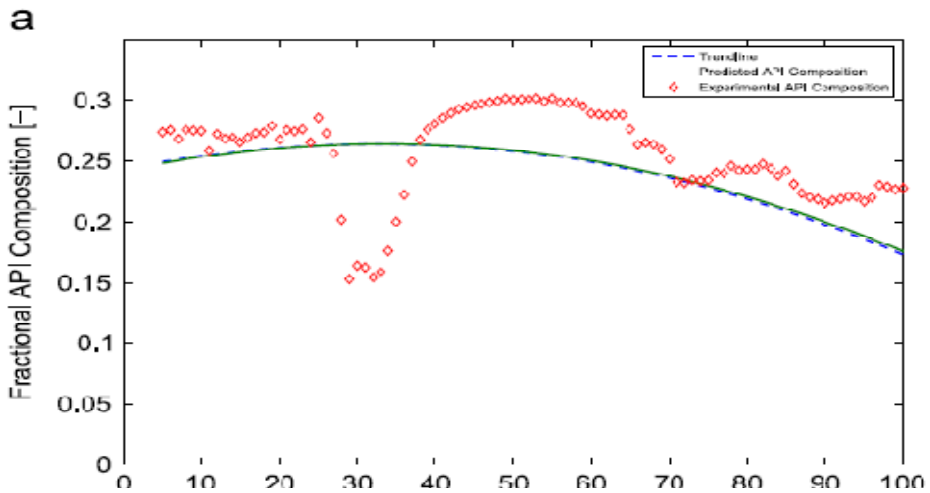

Figure 2(a): Fractional API Composition versus Time at mixer outlet

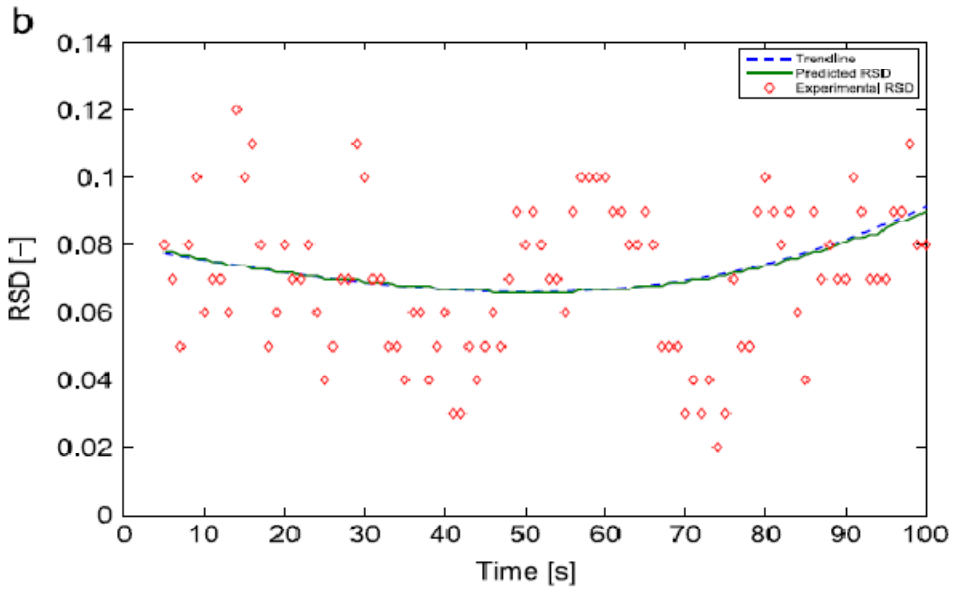

Figure 2(b): RSD versus Time at mixer outlet

In a continuum phase such as a fluid, a perfect steady-state is possible because the inlet and outlet flowrates can match exactly, which is not possible with discrete particles. Hence the concept of perfect steady state is not realised in powder system. There are several ways in which any two particles can interact with each other as well as with the blender wall. Hence the particle-particle interactions and particle-wall interactions will have a pronounced effect on the powder flow. The idea of perfect steady state is not realized in powder system which is also evident from the experimental results. In case of powders, the output fluctuates about a mean. [14, 88] In this case, the simulation has been run for few minutes and the dynamics of the blender over the entire simulation time has been studied. The initial data can be removed (where the fluctuations are more), but in this study all the data points have been retained.

6.1. Fractional API Composition and RSD

The model has been validated for four experimental data sets. Each experimental set provides with data for RSD and API Composition. A linearity test has also been conducted for each case by plotting model predicted data versus experimental data.

6.1.1. Experiment 1

This data set has been obtained for a feed rate of 20 kg/ hr and blender speed of 40 RPM. Figure 2(a) and Figure 2(b) show the comparison between the experimental and model predicted values of API composition and RSD respectively. Figure 3(a) represents the linearity relationship between the experimental and model predicted data for API

composition. Figure 3(b) represents the linearity relationship between the two data sets for RSD. Table 1 gives the value of the statistical parameters.

As shown in Figure 2(a), the predicted API composition is matching exactly with the experimental data (trend line) with very minor error. This can be further verified with the linearity plot as shown in Figure 3(a), where a straight line between predicted API composition and experimental data can be seen. It is reflected in statistical analysis (see Table 1) as well. The R value is found to be 0.999805 indicating that the predicted API composition has a very strong linear relationship (straight line) with the experimental API composition. High value of R^2 (0.999388) and adjusted R^2 (0.99382) indicates a very high certainty in prediction of API composition. A very low value of SSE (0.000176) and SSR (0.001341) further verifies the accuracy of the model. Fig. 2(b) as well as statistical analysis (see Table 1) shows that the model is tracking the experimental RSD data (trend line) very well. Furthermore, Figure 3(b) as well as the statistical analysis indicates that the predicted RSD and experimental RSD have a strong linear relationship (R= 0.999411). Value of R^2 (0.998497) and adjusted R^2 (0.998482) are very high which means that through this model RSD could be predicted with high certainty. In this case the change in the initial and final values of RSD and API composition over the entire time period are 18.05% and 30.5% respectively.

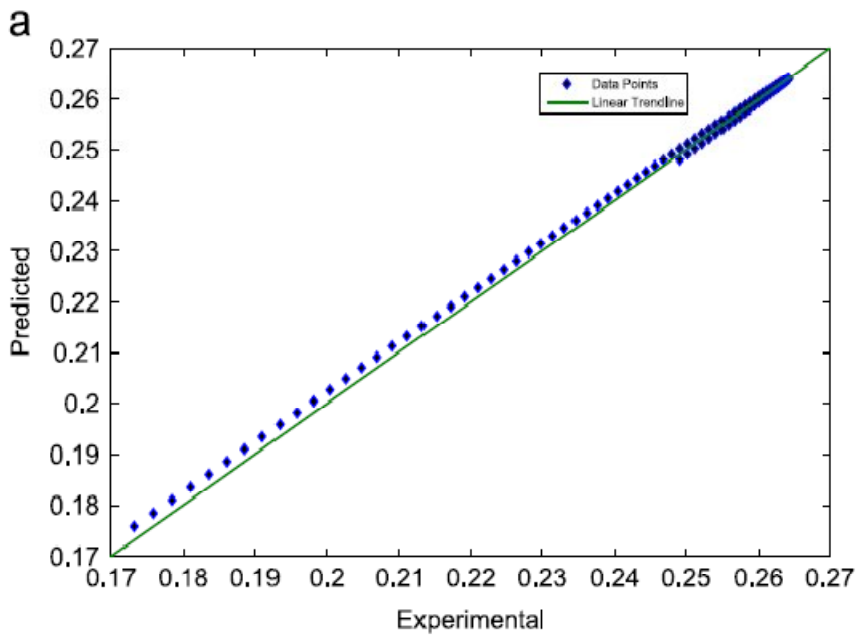

Figure 3(a): Linearity plot of experimental versus predicted data for API composition

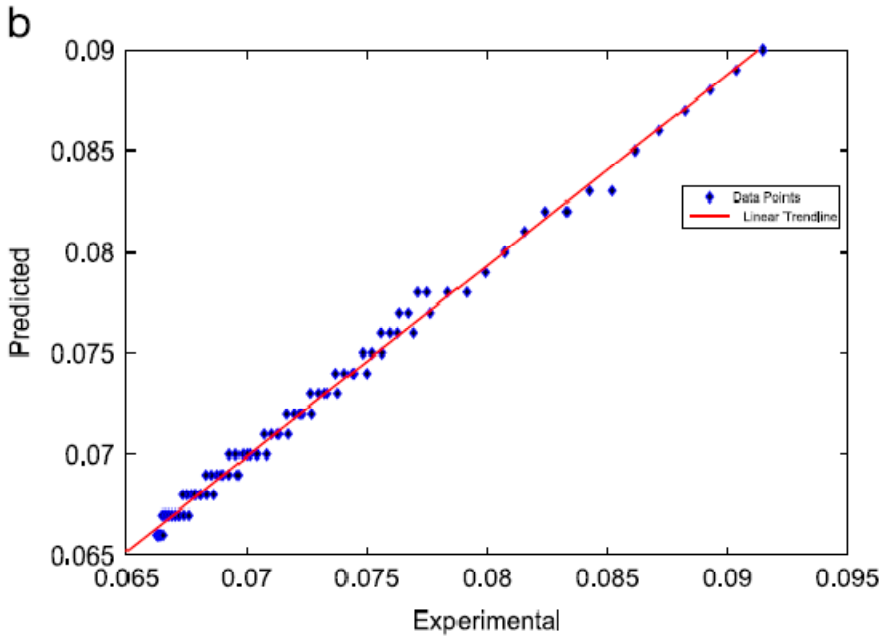

Figure 3(b): Linearity plot of experimental versus predicted data for RSD

API Composition	
Correlation	0.999805
R^2	0.999388
Adjusted R^2	0.99382
SSR	0.001341
SSE	0.000176
Relative Standard Deviation (RSD)	
Correlation	0.999411
R^2	0.998497
Adjusted R^2	0.998482
SSR	0.000607
SSE	3.61 E-5

Table 1: Statistics for experimental set-1

6.1.2. Experiment 2

This data set has been obtained for a feed rate of 20 kg/ hr, blender speed of 200 RPM but with the API concentration of 5%. Figure 4(a) and Figure 4(b) represent the comparison for API composition and RSD respectively. Figure 5(a) and Figure 5(b) show the linearity relationship for API composition and RSD respectively. Table 2 gives the value of the statistical parameters. As desired for a good model, the values of R (0.999366), R^2 (0.997179) and adjusted R^2 (0.997151) are very close to unity while the values of SSR (0.003026) and SSE (0.000897) are very close to zero. Similarly, predicted RSD and experimental RSD (trend line) have a good agreement as shown in Figure 4(b). Figure 5(b) shows a good linear relationship between predicted and experimental RSD. Statistical analysis further verifies strong linearity (R= 0.999346), good RSD prediction certainty (R^2= 0.998425, adjusted R^2= 0.998409) and a good model fitting (SSR= 0.003148, SSE= 0.000971). In this case, the change in the initial and final values of RSD and API values over the entire time period are 44.4% and 41.43% respectively.

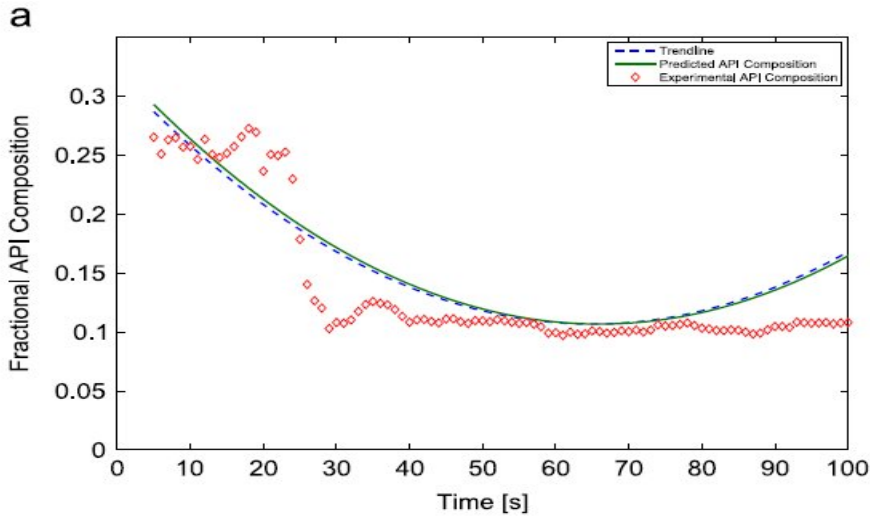

Figure 4(a): Fractional API composition versus time at mixer outlet

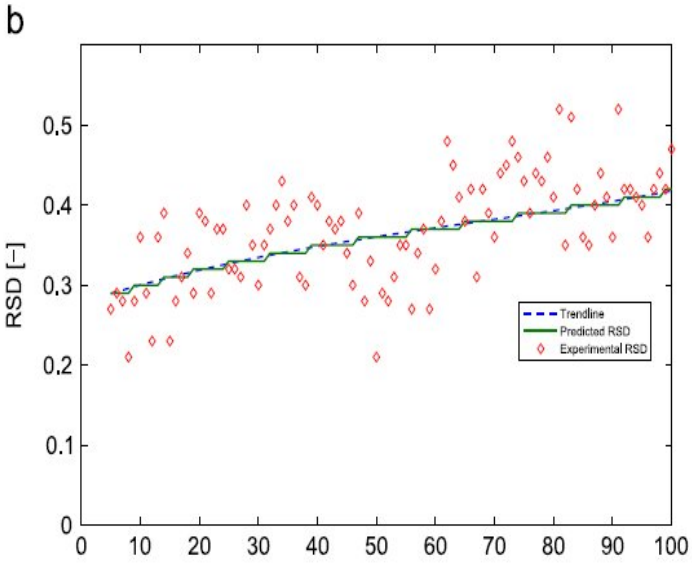

Figure 4(b): Fractional RSD versus time at mixer outlet

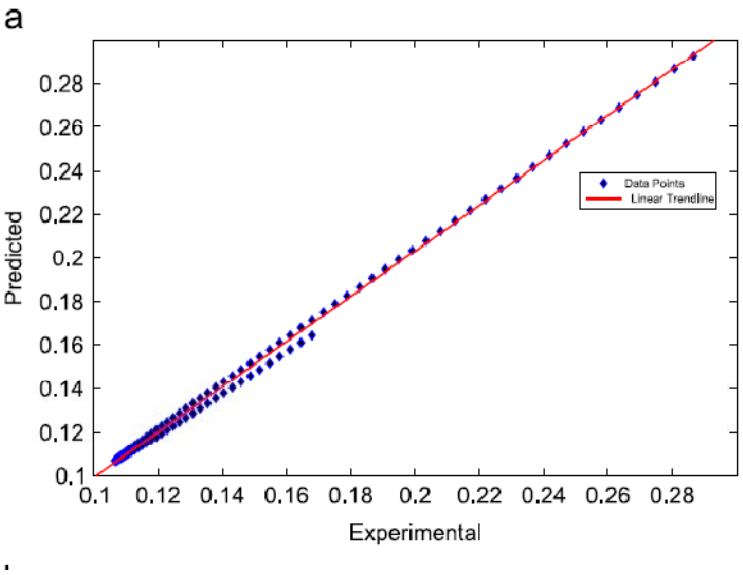

Figure 5(a): Linearity plot between experimental and predicted values for API composition

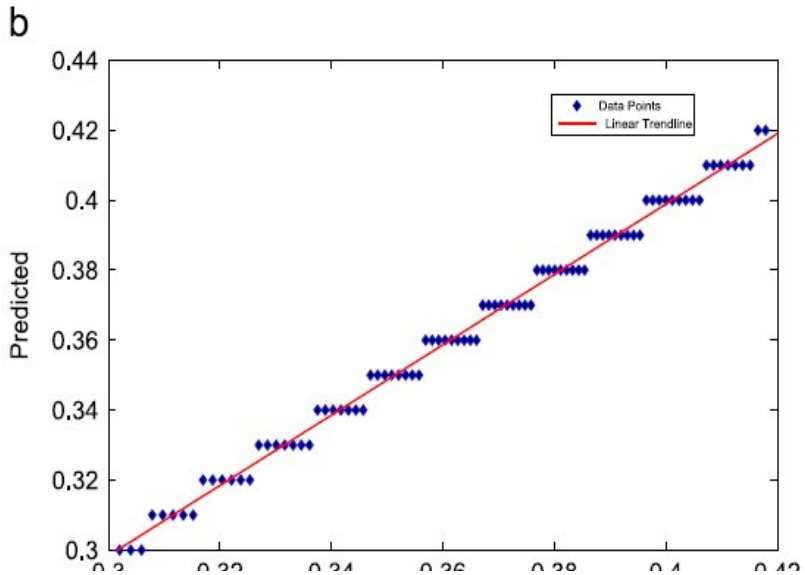

Figure 5(b): Linearity plot between experimental and predicted values for RSD

API Composition	
Correlation	0.999366
R^2	0.997179
Adjusted R^2	0.997151
SSR	0.003026
SSE	0.000897
Relative Standard Deviation (RSD)	
Correlation	0.999346
R^2	0.998425
Adjusted R^2	0.998409
SSR	0.0003148
SSE	0.000971

Table 2: Statistics for experimental set-2

6.1.3. Experiment 3

Another experimental trial has been repeated for the same blender speed of 200 RPM maintaining the feed rate at 20 kg/hr. Figure 6(a) is a comparison of the experimental and model predicted data for API composition and Figure 6(b) is the plot for RSD. Figure 7(a) and Figure 7(b) are the plots of linearity relationship for API composition and RSD respectively. Table 3 gives the value of the statistical parameters. Very high values of R (0.998423), R^2 (0.996064) and adjusted R^2 (0.996024) and very low values of SSR (0.001232), SSE (0.000149) shows a good fit of the mathematical model as well as high certainty in prediction of API composition. The match of predicted RSD with the experimental data can be seen in Figure 6(b) where a small deviation from the trend line has been observed. The statistical analysis (see Table 3) also reflects this. Values of R^2 (0.656826) and adjusted R^2 (0.653324) indicate an average certainty in prediction of RSD. Figure 7(a) represents the linearity relationship between the experimental and model predicted data for API composition. Figure 7(b) represents the linearity relationship between the two datasets for RSD. In this case the change in the initial and final values RSD and API values over the entire time period are 0.00046% and 0.36% respectively. Since several data points are repeated over time, hence an average of the values has been taken to represent the linearity relationship.

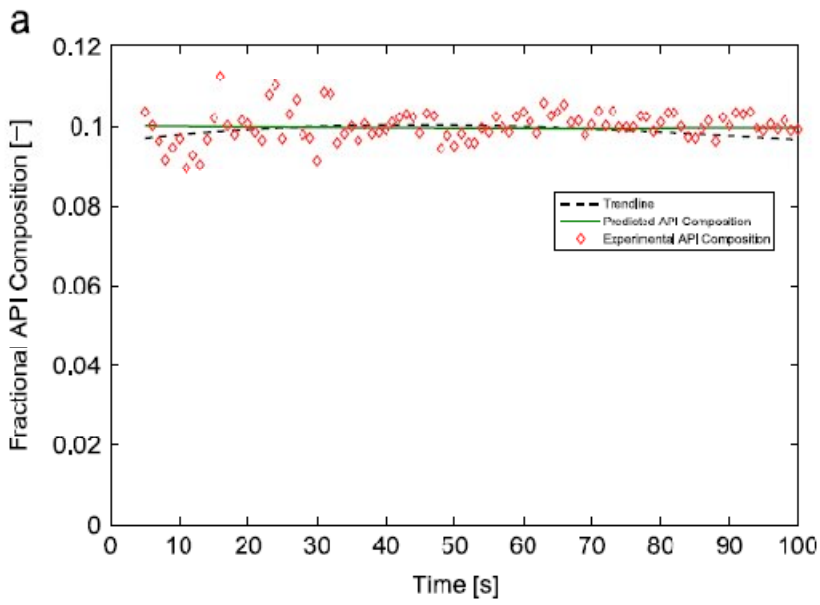

Figure 6(a): Fractional API composition versus time at mixer outlet

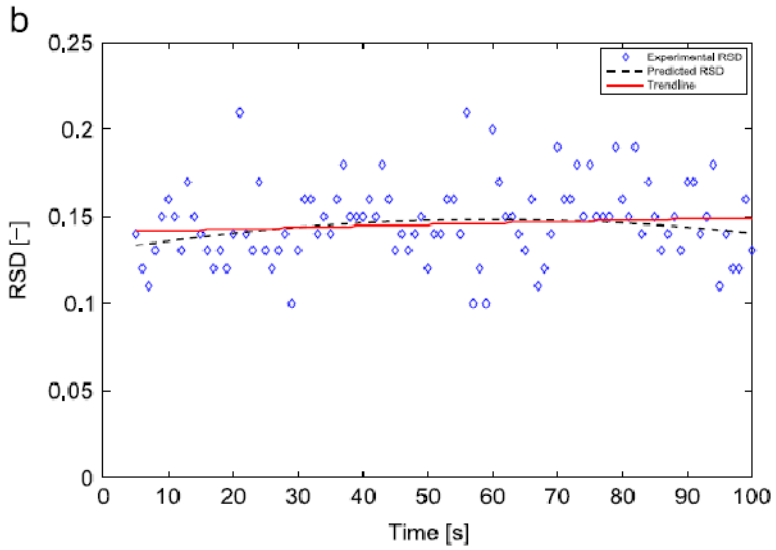

Figure 6(b): RSD versus time at mixer outlet

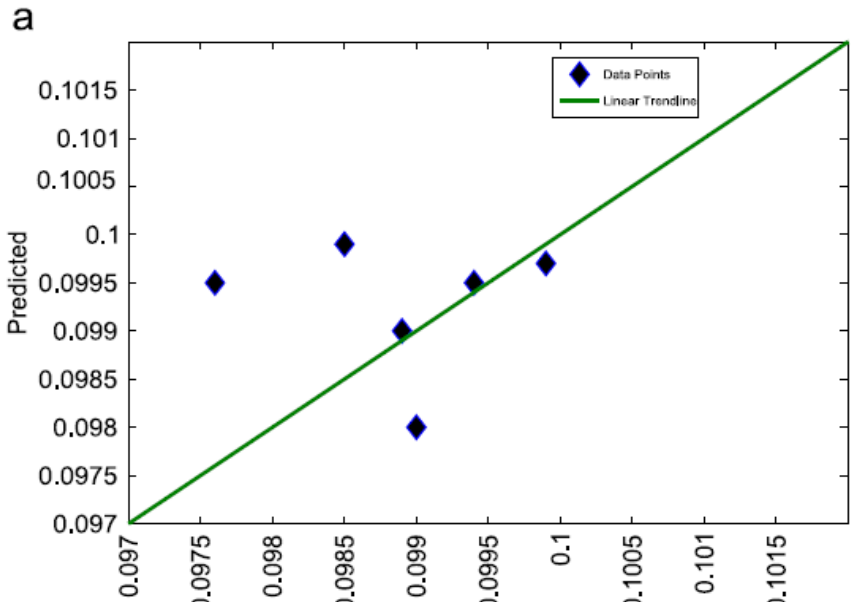

Figure 7(a): Linearity plot between experimental and predicted values for API composition

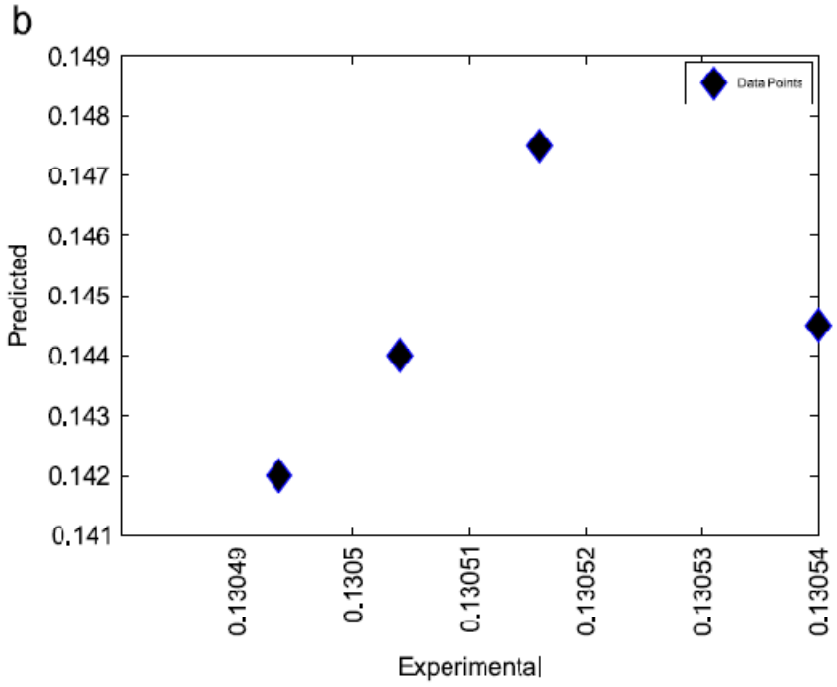

Figure 7(b): Linearity plot between experimental and predicted values for RSD

API Composition	
Correlation	0.998423
R^2	0.996064
Adjusted R^2	0.996024
SSR	0.001232
SSE	0.000149
Relative Standard Deviation (RSD)	
Correlation	0.996931
R^2	0.656826
Adjusted R^2	0.653324
SSR	0.15131
SSE	0.022438

Table 3: Statistics for experimental set-3

6.1.4. Experiment 4

This data set has been obtained for a feed rate of 20 kg/ hr, blender speed of 320 RPM. Figure 8(a) and Figure 8(b) are the plots for API composition and RSD as obtained experimentally and predicted from the model. Figure 9(a) and Figure 9(b) show the linearity relationship for API composition and RSD respectively. Table 4 gives the value of the statistical parameters. In this case also, several data points are repeated over time, hence an average of the values have been taken to represent the linearity relationship. Relationship between the experimental and model predicted data for API composition. Figure 7(b) represents the linearity relationship between the two datasets for RSD. In this case the change in the initial and final values RSD and API values over the entire time period are 0.00046% and 0.36% respectively. Since several data points are repeated over time, hence an average of the values has been taken to represent the linearity relationship.

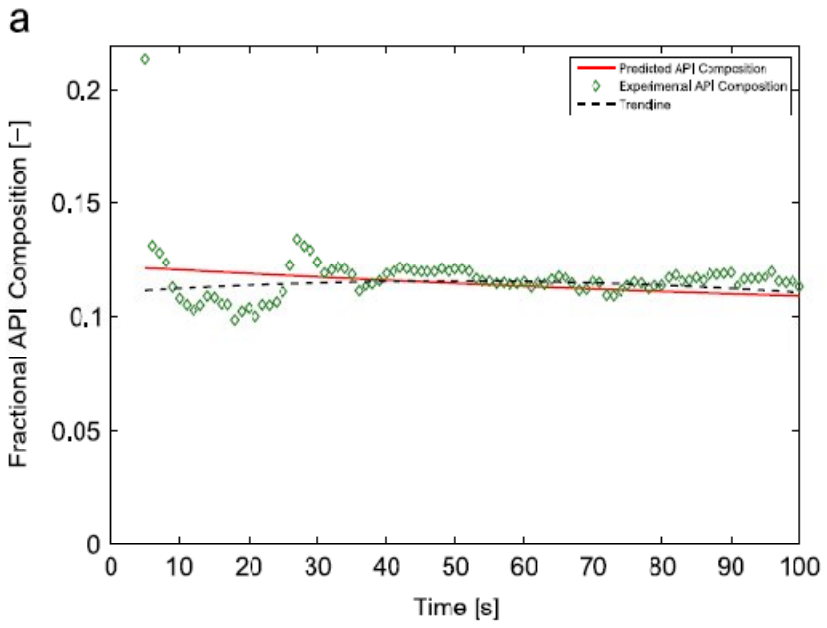

Figure 8(a): Fractional API composition versus time at mixer outlet

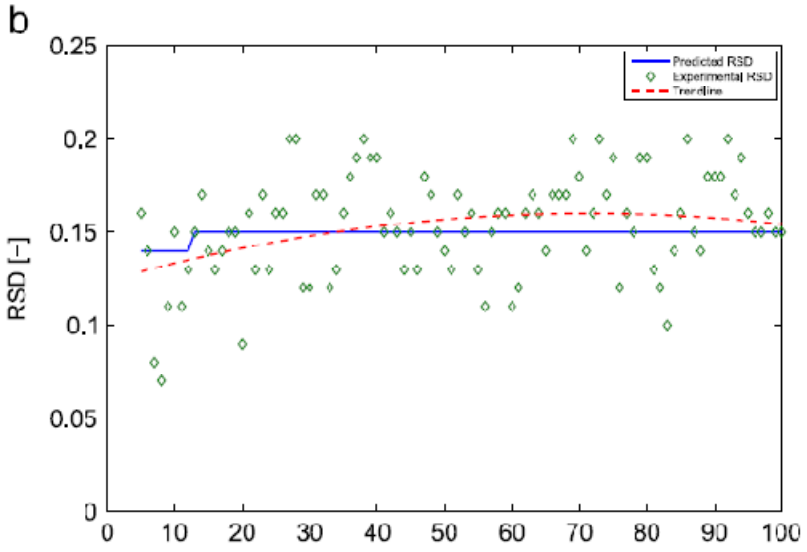

Figure 8(b): RSD versus time at mixer outlet

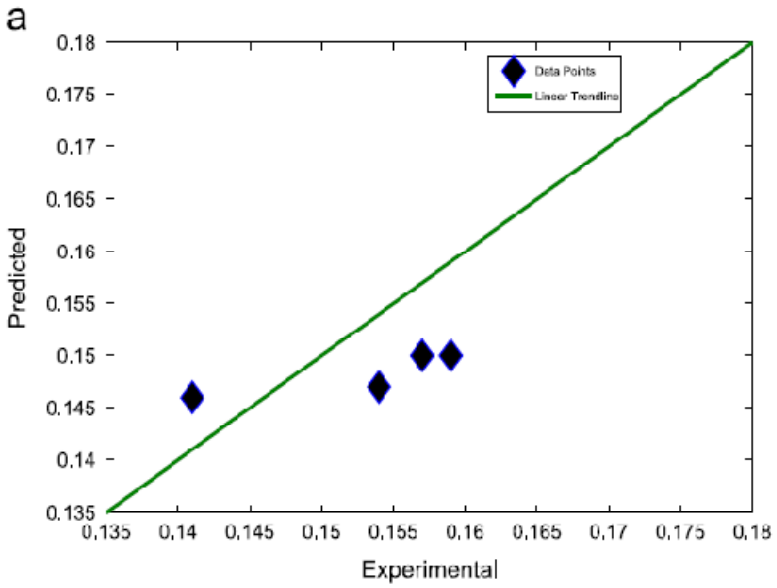

Figure 9(a): Linearity plot between experimental and predicted values for API composition

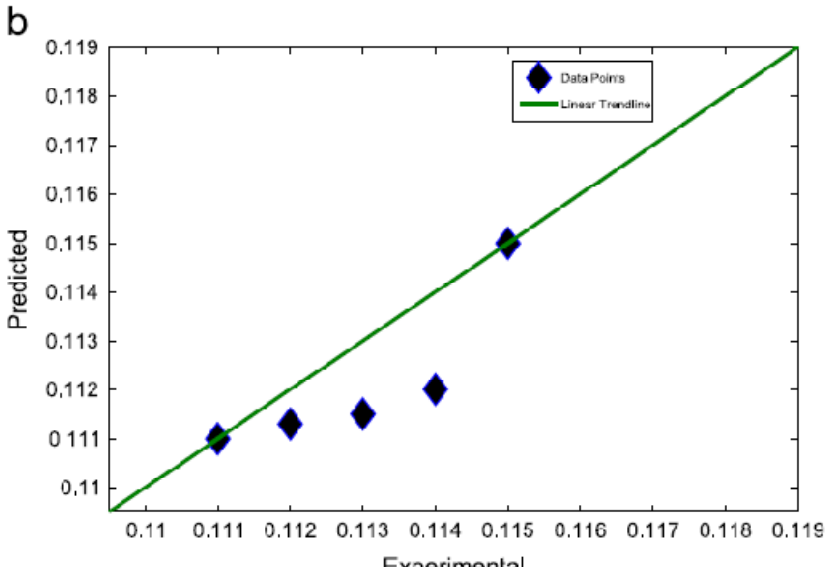

Figure 9(b): Linearity plot between experimental and predicted values for RSD

API Composition	
Correlation	0.987291
R^2	0.973382
Adjusted R^2	0.973111
SSR	0.00369
SSE	0.001355
Relative Standard Deviation (RSD)	
Correlation	0.974142
R^2	0.940338
Adjusted R^2	0.939729
SSR	0.007651
SSE	0.005737

Table 4: Statistics for experimental set-4

6.2. Residence Time Distribution

RTD study was conducted for blender speed of 254 RPM at two different feed rates.

6.2.1 Experiment 1

The blender speed is 254 RPM and feed rate is maintained at 30 kg/hr. Figure 10 shows the comparison between the experimental and predicted data. Figure 11 is the linearity plot. Table 5 gives the statistics of the model.

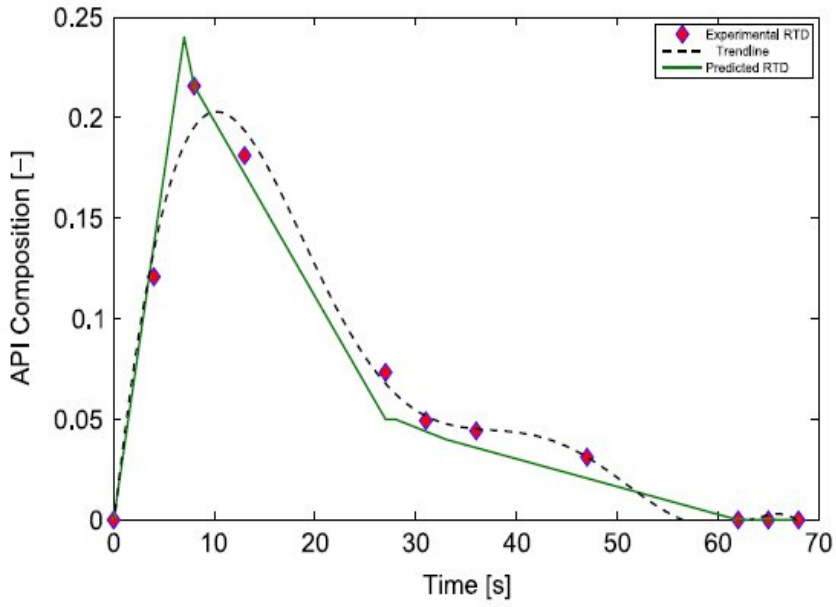

Figure 10: RTD versus time for a feed rate of 30 kg/hr

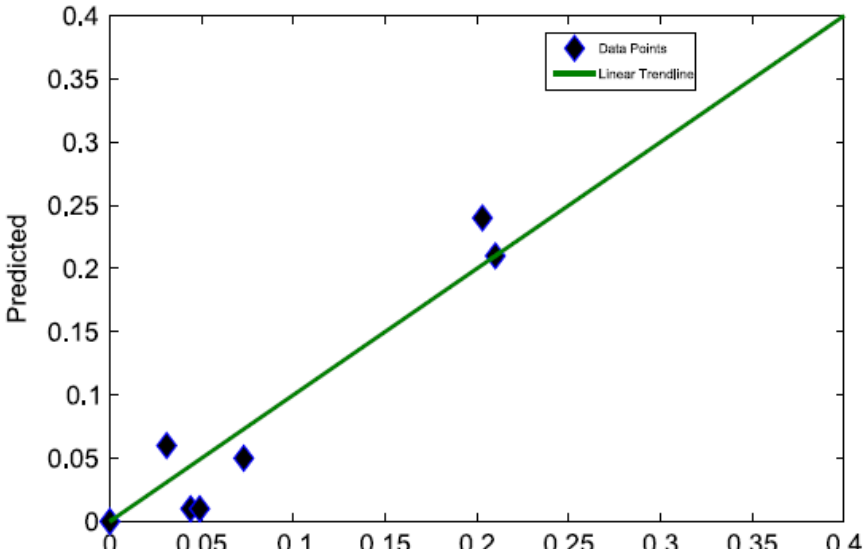

Figure 11: Linearity plot for RTD at a feed rate of 30 kg/hr

RTD	
Correlation	0.815995
R^2	0.540216
Adjusted R^2	0.494238
SSR	0.058952
SSE	0.034753

Table 5: Statistics of RTD run-1

6.2.2 Experiment 2

The blender speed is kept as 254 RPM whereas the feed rate is increased to 45 kg/hr. Figure 12 gives the comparison between the experimental and predicted data. Figure 13 is the linearity plot. Table 6 gives the statistics of the model.

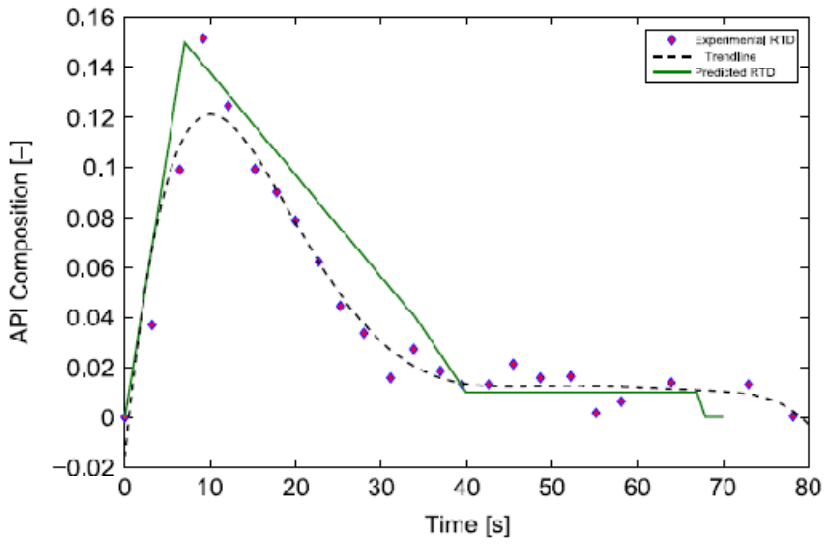

Figure 12: RTD versus time for a feed rate of 45 kg/hr

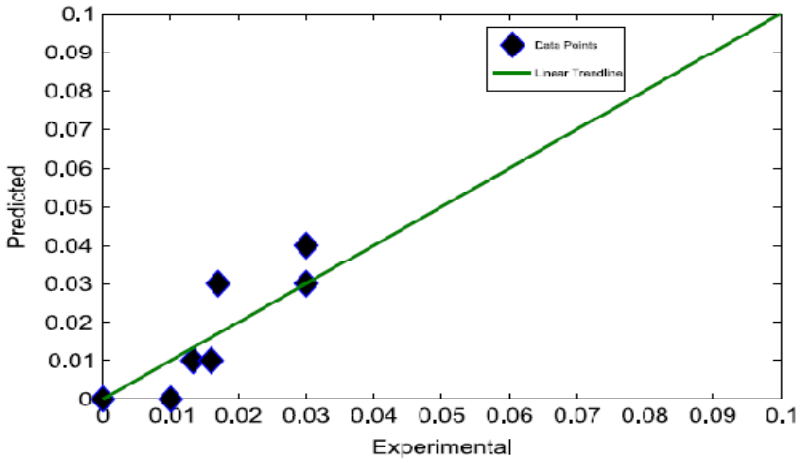

Figure 13: Linearity plot for RTD at a feed rate of 45 kg/hr

RTD	
Correlation	0.831781
R^2	0.625658
Adjusted R^2	0.57218
SSR	0.028012
SSE	0.005493

Table 6: Statistics of RTD run-2

Chapter 7

Conclusion

The aim of this study is validation of the model with experimental results. The parameter values have not been reported because there are 5000 parameters estimated in each experiment. The parameters estimated are the fluxes: Forward flux (F_f), backward flux (F_b) and radial flux (F_r). The dimensions of fluxes are given as:

Number of time step x Number of components x Number of axial compartments x Number of radial compartments= 100 x 2 x 5 x 5=5000.

So there are 5000 parameters to be estimated for each experimental set. It is difficult to report 5000 parameters for each set. Table 7 gives an example of the parameter value estimations(for only the first five sets) for Experiment 3.

F_f (Absolute Magnitude)	F_b (Absolute Magnitude)	F_r (Absolute Magnitude)
0.009	0.02	0.052
0.01	0.02	0.049
0.008	0.02	0.050
0.01	0.02	0.051
0.009	0.02	0.047

Table 7: Parameter values for Experiment 3 for the first five sets.

API composition and RSD have been validated together whereas RTD has been validated separately. This is because the two experiments are conducted in different manner. In case of RTD experiment, API is injected as pulse whereas under normal operational

schedule, both API and excipient are allowed to run simultaneously. The flux ratios obtained in two cases are different. Flux ratios can be defined as the ratio of fluxes of any two compartments between which particle transfer is taking place. It is also a function of the total number of particles being exchanged between the compartments. Hence the parameter values obtained from RSD/API composition and RTD are different.

The parameter values may vary as a function of flow rate and speed. But the authors [14, 88] would not comment on the exact trend of variation with change in flow rate and speed due to absence of enough experiments conducted under different conditions. A proper DOE should be constructed with experiments done under different flow rate conditions and blender speed to be able to come up with an exact trend of variation. The aim of this work is to validate the model only.

A multi-dimensional population balance model (PBM) for mixing has been developed and validated. PBM has been shown to be an effective tool for tracking the blending dynamics in terms of the key properties such as API composition and RSD. The optimization framework developed is dynamic. It is shown to be able to track several experimental runs taken by varying the process parameters. The flux ratios between any two compartments have been optimized. This proves that the model is robust. The statistical analysis showed that the model predicted data matched well with the experimental data and showed high prediction accuracy.

The developed model has wide range of applications in continuous pharmaceutical manufacturing process. Future work includes the integration of mixing model in continuous tablet manufacturing process as well as design and implementation of process monitoring and control system for the same.

Bibliography

[1] S. D. Schaber, D. I. Gerogiorgis, R. Ramachandran, J. M. B. Evans, P. I. Barton, B. L. Trout, 2011.Economic analysis of integrated continuous and batch pharmaceutical manufacturing: a case study.Ind.Eng.Chem.Res.50, 10083–10092.

[2] M. Sen, R. Singh, A. Varanase, **J. John**, R. Ramachandran, Multi-dimensional population balance modeling and experimental validation of continuous powder mixing processes. Chemical Engineering Science 80 (2012) 349–360.

[3] G. V. Reklaitis, J. Khinast, F. J. Muzzio, Pharmaceutical engineering science- new approaches to pharmaceutical development and manufacturing, Chemical Engineering Science 65 (2010) 4 – 7.

[4] A. Gorsek, P. Glavic, Design of batch versus continuous processes: part 1: Single-purpose equipment, Chemical Engineering Research and Design 75 (1997) 709 – 717.

[5] H. Leuenberger, New trends in the production of pharmaceutical granules: Batch versus continuous processing, European Journal of Pharmaceutics and Biopharmaceutics 52 (2001) 289 – 298.

[6] B. Remy, Granular flow, segregation and agglomeration in bladed mixers, Ph.D. thesis, Rutgers, The State University of New Jersey (2010).

[7] S. Adam, D. Suzzi, C. Radeke, J. G. Khinast, An integrated quality by design (QbD) approach towards design space definition of a blending unit operation by discrete element method (DEM) simulation, European Journal of Pharmaceutical Sciences 42 (2011) 106 – 115.

[8] T. Gracia, G. Cook, R. Nosal, PQLI key topics- criticality, design space and control strategy, Journal of Pharmaceutical Innovation 3 (2008) 60 – 68.

[9] R. Nosal, T. Schultz, PQLI definition of criticality, Journal of Pharmaceutical Innovation 3 (2008) 69 – 78.

[10] R. Lionberger, S. L. Lee, L. Lee, A. Raw, L. X. Yu, Quality by design: Concepts for ANDAs, The AAPS Journal 10 (2008) 268 – 276.

[11] R. Singh, K. V. Gernaey, R. Gani, A software for design, analysis and validation of PAT systems, Computers and Chemical Engineering 34 (2010) 1108 – 1136.

[12] L. Yu, Pharmaceutical quality by design: Product and process development, understanding and control, Pharmaceutical Research 25 (2008) 781 – 791.

[13] R. Singh, K. V. Gernaey, R. Gani, Model-based computer-aided framework for design of process monitoring and analysis systems, Computers and Chemical Engineering 33 (2009) 22 –42.

[14] M. Sen, A. Chaudhury, R. Singh, J. John, R. Ramachandran, 2013, Multi-scale flowsheet simulation of an integrated continuous purification-downstream pharmaceutical manufacturing process, International Journal of Pharmaceutics 445, 29-38.

[15] J. Glassey, K. V. Gernaey, C. Clemens, T. W. Schulz, R. Oliveira, G. Striedner, C. F. Mandenius, Process analytical technology (PAT) for biopharmaceuticals, Biotechnology Journal 6 (2011) 369 – 377.

[16] K. Plumb, Continuous processing in the pharmaceutical industry: Changing the mindset, Chemical Engineering Research and design 83 (2005) 730 – 738.

[17] R. Ramachandran, J. Arjunan, A. Chaudhury, M. Ierapetritou, Model-based control-loop performance assesment of a continuous direct compaction pharmaceutical process, Journal of Pharmaceutical Innovation 6 (2011) 249–263.

[18] M. Sen, A. Rogers, R. Singh, A. Chaudhury, , J. John, M. G. Ierapetritou, R. Ramachandran, Flowsheet optimization of an integrated continuous purification processing pharmaceutical manufacturing operation, Submitted to Chemical Engineering Journal, February 2013.

[19] H. Leuenberger, G. Betz, Granulation process control-production of pharmaceutical granules: The classical batch concept and the problem of scale-up, Granulation, Vol. 98, 2007.

[20] F. Boukouvala, M. G. Ierapetritou, Simulation based optimization of expensive flowsheet models for continuous pharmaceutical manufacturing, 2012.

[21] R. Singh, M. Ierapetritou, R. Ramachandran, 2012. An engineering study on the enhanced control and operation of continuous manufacturing of pharmaceutical tablets via roller compaction. Int. J. Pharm 438, 307 – 326.

[22] H. Leuenberger, Scale-up in the 4th dimension in the field of granulation and drying or how to avoid classical scale-up, Powder Technology 130 (2003) 225 – 230.

[23] J. Werani, M. Grunberg, C. Ober, H. Leuenberger, Semicontinuous granulation- the process of choice for the production of pharmaceutical granules, Powder Technology 140 (2004) 163 –168.

[24] G. Betz, P. Junker-Purgin, H. Leuenberger, Batch and continuous processing in the production of pharmaceutical granules., Pharmaceutical Development and Technology 8 (2003) 289 – 297.

[25] A. Gorsek, P. Glavic, Design of batch versus continuous processes:part 2:multi-purpose equipment, Trans IChemE 75 (1997) 709 – 717.

[26] K. R. Wilburn, The business case for continuous manufacturing of pharmaceuticals, Ph.D. thesis, MIT (2010).

[27] R. Singh, R. Rozada-Sanchez, T. Wrate, F. muller, K. V. Gernaey, R. Gani, J. M. Woodley, Fast, flexible, future (F3), pharmaceutical production processes, Computer Aided Chemical Engineering 29 (2010) 291 – 295.

[28] M. Sen, R. Ramachandran, 2012. A multi-dimensional population balance model approach to continuous powder mixing processes. Advanced powder technology, doi:10.1016/j.apt.2012.02.001.

[29] K. V. Gernaey, R. Gani, A model-based systems approach to pharmaceutical product process design and analysis, Chemical Engineering Science 65 (2010) 5757 – 5769.

[30] K. U. Klatt, W. Marquardt, Perspectives of process systems engineering-personal views from academia and industry., Computers and Chemical Engineering 33 (2009) 536 – 550.

[31] F. Boukoulava, F. J. Muzzio, M. G. Ierapetritou, Design space of pharmaceutical processes using data-driven-based methods, Journal of Pharmaceutical Innovation 5 (2010) 119 – 137.

[32] O. S. Sudah, A. W. Chester, J. A. Kowalski, J. W. Beeckman, F. J. Muzzio, Quantitative characterization of mixing processes in rotary calciners, Powder Technology 126 (2002) 166 –173.

[33] H. Wu, E. J. Heilweil, A. S. Hussain, M. A. Khan, Process analytical technologies (PAT)- effects of instrumental and compositional variables in terahertz spectral data quality to characterize pharmaceutical materials and tablets, Computer Aided Chemical Engineering 343 (2007) 148– 158.

[34] P. M. Portillo, F. J. Muzzio, M. G. Ierapetritou, Characterizing powder mixing processes utilizing compartment models, International Journal of Pharmaceutics 14 (2006) 320.

[35] H. Berthiaux, K. Marikh, V. Mizonov, D. Ponomarev, E. Barantzeva, Modeling continuous powder mixing by means of markov chains, Particulate Science and Technology 22 (2004) 379– 389.

[36] P. M. Portillo, M. G. Ierapetritou, F. J. Muzzio, Effects of rotation rate, mixing angle, and cohesion in two continuous powder mixers–a statistical approach, Powder Technology 194 (2009) 217 – 227.

[37] P. M. Portillo, F. J. Muzzio, M. G. Ierapetritou, Using compartment modeling to investigate mixing behavior of a continuous mixer, Journal of Pharmaceutical Innovation 3 (2008) 161 –174.

[38] Y. Gao, F. Muzzio, M. G. Ierapetritou, Characterization of feeder effects on continuous solid mixing using fourier series analysis, AIChE Journal 57 (2011) 1144 – 1153.

[39] Y. Gao, F. Muzzio, M. G. Ierapetritou, Investigation on the effect of blade patterns on continuous solid mixing performance, The Canadian Journal of Chemical Engineering 89 (2010) 969 – 984.

[40] Y. Gao, A. Vanarase, F. Muzzio, M. G. Ierapetritou, Characterizing continuous powder mixing residence time distribution, Chemical Engineering Science 66 (2011) 417 – 425.

[41] A. Vanarase, M. Alcal, J. Rozo, F. Muzzio, R. Romaach, Real-time monitoring of drug concentration in a continuous powder mixing process using NIR spectroscopy, Chemical Engineering Science 65 (21) (2010) 5728 – 5733.

[42] W. R. Ketterhagen, M. T. Ende, B. C. Hancock, B. Hancock, Process modeling in the pharmaceutical industry using the discrete element method, Journal of Pharmaceutical Sciences 98 (2009) 442 – 470.

[43] P. M. Portillo, F. J. Muzzio, M. G. Ierapetritou, Hybrid DEM-compartment modeling. Approach for granular mixing, AICHE Journal 53 (2007) 119 – 128.

[44] B. Freirich, J. Li, J. D. Lister, C. Wassgren, Incorporating particle flow information from discrete element simulations in population balance models of mixer coaters, Chemical Engineering Science 66 (2011) 3592 – 3604.

[45] M. Sen, A. Dubey, R. Ramachandran, Quantitative development and validation of a hybrid multi-dimensional population balance model describing a continuous powder mixing process, Submitted to Chemical Engineering Research and Design.

[46] A. Sarkar, C. Wassgren, Continuous blending of cohesive granular material, Chemical Engineering Science 65 (2010) 5687 – 5698.

[47] A. Sarkar, C. Wassgren, Effect of operating conditions on flow and mixing, Chemical Engineering Science 64 (2009) 2672 – 2682.

[48] F. Bertrand, L. Leclaire, G. Levecque, DEM-based models for the mixing of granualar materials, Chemical Engineering Science 60 (2005) 2517 – 2531.

[49] A. Dubey, A. Sarkar, M. Ierapetritou, C. Wassgren, F. Muzzio, Computational approaches for studying the granular dynamics of continuous blending processes, 1 DEM based methods, Macromolecular Materials and Engineering 296 (2011) 290 – 307.

[50] F. Boukouvala, A. Dubey, A. Vanarase, R. R. anf F J Muzzio, M. Ierapetritou, Computational approaches for studying the granular dynamics of continuous blending processes, 2 population balance and data-based methods, Computer Aided Chemical Engineering 297 (2012) 9 – 19.

[51] B. Remy, J. Khinast, B. Glasser, Discrete element simulation of free flowing grains in a four- bladed mixer, AICHE Journal 55 (2009) 2035 – 2058.

[52] B. Remy, T. M. Canty, J. G. Khinast, B. J. Glasser, Experiments and simulations of cohesionless particles with varying roughness in a bladed mixer, Chemical Engineering Science 65 (2010) 4557 – 4571.

[53] B. Remy, B. J. Glasser, The effect of mixer properties and fill level on granular flow in a bladed mixer, AICHE Journal 56 (2010) 336 – 353.

[54] A. Hassanpour, H. Tan, A. Bayly, P. Gopalakrishna, B. Ng, M. Ghadiri, Analysis of particle motion in a paddle mixer using discrete element method (dem), Powder Technology 206 (2011) 189 – 194.

[55] Y. Tsuji, T. Kawaguchi, T. Tanaka, Discrete particle simulation of 2-dimensional fluidized-bed, Powder Technology 77 (1993) 79 – 87.

[56] B. H. Xu, A. B. Yu, Numerical simulation of the gas-solid flow in a fluidized bed by combining discrete particle method with computational fluid dynamics, Chemical Engineering Science 53 (1997) 2646 – 2647.

[57] H. Zhu, Z. Zhouand, R. Yang, A. Yu, Discrete particle simulation of particulate systems: Theoretical developments, Chemical Engineering Science 62 (2007) 3378 – 3392.

[58] M. Moakher, T. Shinbrot, F. Muzzio, Experimentally validated computations of flow, mixing and segregation of non-cohesive grains in 3D tumbling blenders, Powder Technology 109 (2000) 58 – 71.

[59] H. P. Kuo, R. C. Knight, D. J. Parker, M. J. Adams, J. P. K. Seville, The influence of DEM simulation parameters on the particle behavior in a v-mixer, Chemical Engineering Science 57 (2002) 3621 – 3638.

[60] M. Lemieux, M. Bertrand, J. Chaouki, P. Gosselin, Comparative study of the mixing of free- flowing particles in a v-blender and a bin-blender, Chemical Engineering Science 62 (2007) 1738 – 1802.

[61] O. S. Sudah, P. E. Arratia, A. Alexander, F. Muzzio, Simulation and experiments of mixing and segregation in a tote blender, AICHE Journal 51 (2005) 836 – 844.

[62] P. E. Arratia, N. H. Duong, F. J. Muzzio, P. Godbole, S. Reynolds, A study of the mixing and segregation mechanisms in the bohle tote blender via dem simulations, Powder technology 164 (2006) 50 – 57.

[63] S. Endoh, J. Szepvolgyi, T. Hayashi, M. Naito, T. Tanimoto, Simulation of motion of particles in high speed elliptical-rotor-type mixer by particle element method, Kagaku Kogaku Ronbunshu 26 (2000) 268 – 274.

[64] T. Iwasaki, M. Satoh, T. Koga, Analysis of collision energy of bead media in a high-speed elliptical-rotor-type powder mixer using the discrete element method, Powder technology 121 (2001) 239 – 248.

[65] T. Hotta, M. Naito, J. Szepvolgyi, S. Endoh, K. Nogi, Effect of rotor shape on particle composite process by a high-speed elliptical-rotor-type mixer, Kagaku Kogaku Ronbunshu 27 (2001) 141 – 143.

[66] J. Kano, H. Yabune, H. Mio, F. Saito, Grinding of talc particulates by a high-speed rotor mixer, Advanced Powder technology 12 (2001) 207 – 214.

[67] M. A. I. Schutyser, W. J. Briels, A. Rinzeman, R. M. Boom, Numerical simulation and PEPT measurements of a 3D conical helical-blade mixer, a high potential solids mixer for solid state fermentation, Biotechnology and Bioengineering 84 (2003) 29 – 39.

[68] R. L. Stewart, J. Bridgewater, Y. C. Zhou, A. B. Yu, Simulated and measured flow of granules in a bladed mixer-a detailed comparison, Chemical Engineering Science 56 (2001) 5457 – 5471.

[69] B. Chaudhuri, F. J. Muzzio, M. S. Tomassone, Modeling of heat transfer in granular flow in rotating vessels, Chemical Engineering Science 61 (2006) 6348 – 6360.

[70] B. Yu, Discrete element method: an effective method for particle scale research of particulate matter, Engineering Computations 21 (2004) 205 – 214.

[71] P. Marchal, R. David, J. P. Klein, J. Villermaux, Crystalisation and precipitation engineering- i. an efficient method for solving population balances in crystalisation and agglomeration, Chemical Engineering Science 43 (1988) 59 – 67.

[72] F. Puel, G. Fevotte, J. P. Klein, Simulation and analysis of industrial crystalization processes through multidimensional population equations. part 1: a resolution algorithm based on method of classes, Chemical Engineering Science 58 (2003) 3715 – 3727.

[73] R. Gunawan, I. Fusman, R. D. Bratz, High resolution algorithms for multidimensional population balance equations, AIChE Journal 50 (2004) 2738 – 2749.

[74] D. L. Ma, D. K. Tafti, R. D. Braatz, High-resolution simulation of multidimensional crystal growth, Industrial and Engineering Chemistry Research 41 (2002) 6271 – 6223.

[75] C. D. Immanuel, F. J. Doyle III, Solution technique for a multi-dimensional population balance model describing granulation processes, Powder Technology 156 (2005) 213-225.

[76] J. M. H. Poon, C. D. Immanuel, F. J. Doyle III, J. D. Litster, A three-dimensional population balance model of granulation with a mechanistic representation of the nucleation and aggregation phenomena, Chemical Engineering Science 63 (2008) 1315 – 1329.

[77] J. M. H. Poon, R. Ramachandran, C. F. W. Sanders, T. Glasser, C. D. Immanuel, F. J. Doyle III, J. D. Litster, F. Stepanek, F. Y. Wang, I. T. Cameron, Experimental validation studies on a multi-scale and multi-dimensional population balance model of batch granulation, Chemical Engineering Science 64 (2009) 775 – 786.

[78] R. Ramachandran, C. D. Immanuel, F. Stepanek, J. D. Litster, F. J. Doyle III, A mechanistic model for granule breakage in population balances of granulation: theoretical kernel development and experimental validation, Chemical Engineering Research and Design 87 (2009) 598 – 614.

[79] R. Ramachandran, P. I. Barton, Effective parameter estimation within a multi-dimensional population balance model framework, Chemical Engineering Science 65 (2010) 4884 – 4893.

[80] F. Stepanek, P. Rajniak, C. Mancinelli, R. T. Chern, R. Ramachandran, Distribution and accessibility of binder in wet granules, Powder Technology 189 (2009) 376 – 384.

[81] R. Ramachandran, A. Chaudhury, Model-based design and control of continuous drum granulation processes, Chemical Engineering Research & Design Accepted (2011) doi:10.1016/j.cherd.2011.10.022.

[82] R. Ramachandran, M. A. Ansari, A. Chaudhury, A. Kapadia, A. V. Prakash, F. Stepanek, A quantitative assessment of the influence of primary particle size distribution on granule inhomogeneity, Chemical Engineering Science Accepted (2011) doi: 10.1016/j.ces.2011.11.045.

[83] R. Ramachandran, J. M. H. Poon, C. F. W. Sanders, T. Glaser, C. D. Immanuel, F. J. D. III, J. D. Litster, F. Stepanek, F. Wang, I. T. Cameron, Experimental studies on distributions on granule size, binder content and porosity in batch drum granulation: inferences on process modeling requirements and process sensitivities, Powder Technology 188 (2008) 89–101.

[84] [D. Ramakrishna, Population balances, Academic Press San Diego.

[85] A. Vanarase, F. Muzzio, Effect of operating conditions and design parameters in a continuous powder mixer, Powder Technology 208 (1) (2011) 26 – 36.

[86] A. Drud, A GRG code for large sparse dynamic nonlinear optimization problems, Mathematical Programming 31 (1985) 153 – 191.

[87] A. Drud, Conopt-a large scale GRG code, ORSA Journal on Computing 6 (1992) 207 – 216.

[88] M. Sen, A. Dubey, R. Singh, R. Ramachandran, 2013, Mathematical Development and Comparison of a Hybrid PBM-DEM description of a Continuous Powder Mixing Process, Journal of Powder Technology, in press, http://dx.doi.org/10.1155/2013/843784.

Vita

Joyce John

2013 M.S. in Chemical and Biochemical Engineering, Rutgers University

2010 B. Tech. in Biotechnology Engineering from Calicut University, India

2005 Graduated from Indian Community School, Kuwait.

Publications

1. Maitraye Sen, Ravendra Singh, Aditya Varanase, Joyce John, Rohit Ramachandran, Multi-dimensional population balance modeling and experimental validation of continuous powder mixing processes, Chemical Engineering Science 80 (2012) 349–360.
2. Maitraye Sen, Anwesha Chaudhury, Ravendra Singh, Joyce John, Rohit Ramachandran, 2013, Multi-scale flowsheet simulation of an integrated continuous purification-downstream pharmaceutical manufacturing process, International Journal of Pharmaceutics 445, 29-38.
3. Maitraye Sen, Amanda Rogers, Ravendra Singh, Anwesha Chaudhury, , Joyce John, Marianthi G. Ierapetritou, Rohit Ramachandran, Flowsheet optimization of an integrated continuous purification processing pharmaceutical manufacturing operation, Submitted to Chemical Engineering Journal, February 2013.